Mixed-Valent Spin-Crossover System

An Unprecedented Homochiral Mixed-Valence Spin-Crossover Compound**

Yukinari Sunatsuki, Yuichi Ikuta, Naohide Matsumoto, Hiromi Ohta, Masaaki Kojima, Seiichiro Iijima, Shinya Hayami, Yonezo Maeda, Sumio Kaizaki, Françoise Dahan, and Jean-Pierre Tuchagues*

The phenomenon of spin-crossover between the low-spin (LS) and high-spin (HS) states,[1] which is observed in some octahedral $3d^n$ ($4 \leq n \leq 7$) metal complexes and is induced by an external perturbation, such as temperature, pressure, or light irradiation, is one of the most spectacular examples of molecular bistability.[2,3] Such phenomena can be utilized in new electronic devices, such as molecular memories and switches that are controlled by many different physical channels.[4,5] It is now established that cooperative spin-crossover, the interaction between spin-crossover sites, is the predominant factor governing bistability.[6,7] We now report the first homochiral mixed-valence spin-crossover compound, in which three independent properties are united, namely, mixed valence states of iron metal centers, spin-crossover of the Fe^{II} and Fe^{III} electronic structures, and homochiral assembly of the chiral $[Fe^{II}H_3L]^{2+}$ and $[Fe^{III}L]$ building blocks into a conglomerate structure (H_3L = tris{[2-{(imidazole-4-yl)methylidene}amino]ethyl}amine). Mixed valence states can allow access to several electronic states as a result of spin-crossover in both the Fe^{II} and Fe^{III} centers, and supramolecular assembly can produce a cooperative effect between the spin-crossover sites. Furthermore, optical activity can be used to observe the switching of spin states (reading process).

[*] Prof. Dr. N. Matsumoto, Y. Ikuta
Department of Chemistry, Faculty of Science, Kumamoto University, Kurokami 2-39-1, Kumamoto 860-8555 (Japan)
Fax: (+81) 96-342-3390
E-mail: naohide@aster.sci.kumamoto-u.ac.jp
Dr. Y. Sunatsuki, H. Ohta, Prof. Dr. M. Kojima
Department of Chemistry, Faculty of Science, Okayama University, Tsushima-naka 3-1-1, Okayama 700-8530 (Japan)
Dr. S. Iijima
National Institute of Advanced Industrial Science and Technology, Tsukuba 305-8566 (Japan)
Dr. S. Hayami, Prof. Dr. Y. Maeda
Division of Chemistry, Faculty of Sciences, Kyushu University, Hakozaki, Fukuoka 812-8581 (Japan)
Prof. Dr. S. Kaizaki
Department of Chemistry, Graduate School of Science, Osaka University, Machikaneyama Cho 1-1, Toyonaka 560-0043 (Japan)
Dr. F. Dahan, Prof. Dr. J.-P. Tuchagues
Laboratoire de Chimie de Coordination du CNRS, UP 8241, 205 Route de Narbonne, 31077 Toulouse cedex (France)

[**] This work was supported by a Grant-in-Aid for Science Research (No. 14340209) from the Ministry of Education, Science, Sports, and Culture, Japan, the Fund for Project Research from the Venture Business Laboratory, Graduate School of Okayama University, and the JSPS Research Fellowship for Young Scientists (Y.S.).

  DOI: 10.1002/ange.200250399

Yellow-orange crystals of $[Fe^{II}H_3L](NO_3)_2{\cdot}3H_2O$ were prepared by the reaction of the tripod ligand H_3L and $Fe^{III}(NO_3)_3{\cdot}9H_2O$ in MeOH under acidic conditions, where it should be noted that with this ligand, the Fe^{II} complex is obtained from the Fe^{III} salt. When three equivalents of NaOH solution were added to a solution of $[Fe^{II}H_3L](NO_3)_2{\cdot}3H_2O$ in methanol under aerobic conditions, the color of the solution changed from yellow-orange to blue; the fully deprotonated $[Fe^{III}L]{\cdot}2.5H_2O$ was obtained as blue-black crystals. However, when only 1.5 equivalents of NaOH was added under similar conditions, the color of the solution became green, and the mixed-valence compound, $[Fe^{II}H_3L][Fe^{III}L](NO_3)_2$ (**1**) was obtained. The IR spectrum of **1** showed two intense bands at 1635 and 1603 cm^{-1} that were assigned to the C = N stretching vibration of the Schiff base ligand at room temperature, and are ascribed to the $[Fe^{II}H_3L]^{2+}$ and $[Fe^{III}L]$ species, respectively; the bands are sensitive to the oxidation and spin states of iron in both building units.

The synthetic procedure is schematically drawn in Figure 1. In accordance with what has already been observed for the analogous Co^{III} complex with the tripod ligand,[8] this synthetic procedure gives an example of the evolution of chirality.[9] The coordination of an achiral tripod ligand to a transition-metal ion yields Δ (clockwise) and Λ (anticlockwise) chiral molecules, as a result of a screw coordination arrangement of the ligand. In the iron system, deprotonation and oxidation of the $[Fe^{II}H_3L]^{2+}$ species occurred to generate the fully-deprotonated $[Fe^{III}L]$ species, which functions as a constituent component of the mixed-valence compound. Deprotonation at the imidazole moiety initiates a self-organization process that is associated with intermolecular homochiral discrimination arising from the formation of an imidazole–imidazolate hydrogen bond between the $[Fe^{II}H_3L]^{2+}$ and $[Fe^{III}L]$ species. This process results in the formation of an extended homochiral two-dimensional (2D) sheet, which, in turn, leads to a conglomerate structure, constructed through the homochiral stacking of the 2D sheets.

The crystal structure of **1** was determined at both 295 and 100 K.[10] The structure consists of two pairs of protonated $[Fe^{II}H_3L]^{2+}$ (Fe2 and Fe4) and deprotonated $[Fe^{III}L]$ (Fe1 and Fe3) species, and four nitrate counterions (Figure 2). The $[Fe^{II}H_3L]^{2+}$ and $[Fe^{III}L]$ components with octahedral N_6 coordination environments are chiral species with either the Δ or *Λ* configuration. These components act as chiral complementary building units that assemble together to form a 2D extended sheet arising from the network of imidazole–imidazolate hydrogen bonds. In this 2D supramolecular structure, the capped tripodlike $[Fe^{II}H_3L]^{2+}$ and $[Fe^{III}L]$ components form an alternate "up-and-down" array that yields a homochiral extended 2D puckered sheet based on a hexanuclear unit centered on a trigonal void. In addition, sheets with the same chirality are arranged parallel to each

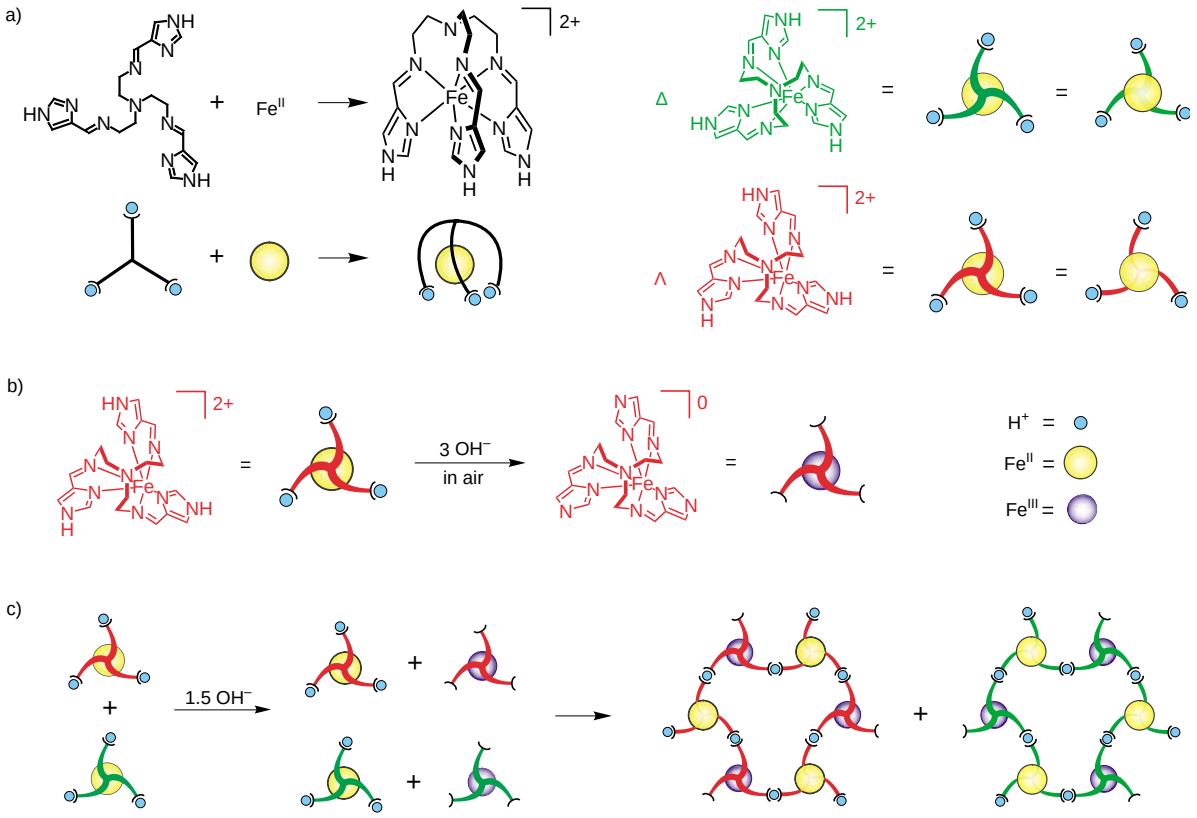

Figure 1. a) Formation of the isolated chiral molecule $[Fe^{II}H_3L]^{2+}$ (Δ and Λ) from the achiral H_3L ligand and an Fe^{II} ion. Schematic drawings are viewed along the molecular C_3 axis; b) deprotonation at the imidazole moieties of $[Fe^{II}H_3L]^{2+}$ in air generates $[Fe^{III}L]$; c) formation of a homochiral assembled hexamer which constitutes a unit of a 2D sheet. The organization process is accompanied by intermolecular homochiral discrimination between $[Fe^{II}H_3L]^{2+}$ and $[Fe^{III}L]$ units to produce an extended homochiral 2D sheet held together by imidazole–imidazolate hydrogen bonds.

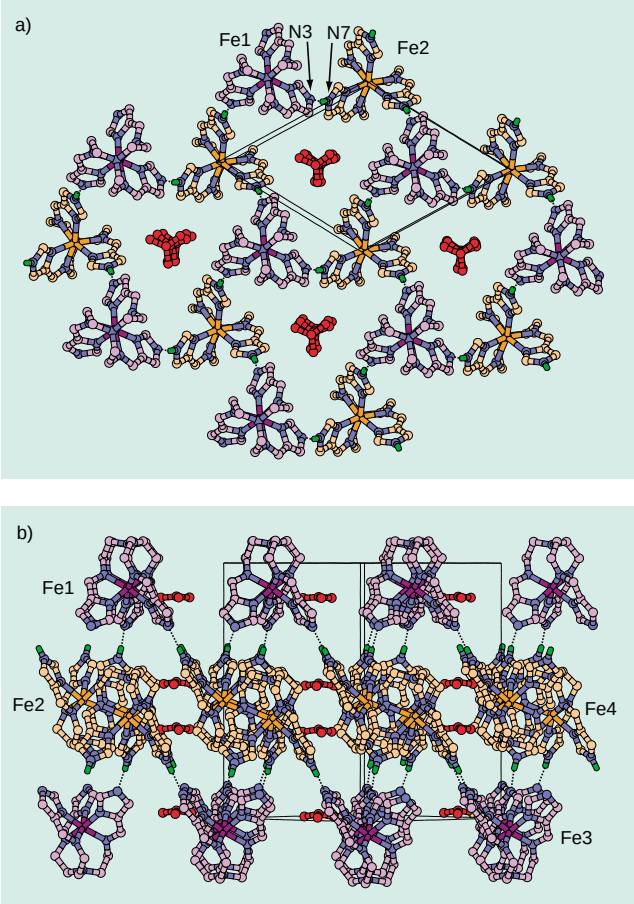

Figure 2. X-ray crystal structure of **1**. a) A view showing the homochiral 2D sheet with trigonal voids. The two complementary molecular building units having the same chirality, that is, the protonated species $[Fe^{II}H_3L]^{2+}$ (Λ enantiomer, orange) and the deprotonated species $[Fe^{III}L]^{0}$ (Λ enantiomer, purple), which are linked by hydrogen bonds and arranged alternately in an up-and-down fashion; b) a side view showing the stacking arrangement of adjacent sheets having the same chirality. Their up-and-down formation favors the stacking of adjacent sheets that have the same chirality along the *c* axis. The nitrate counterions are located in the cavities and between the sheets.

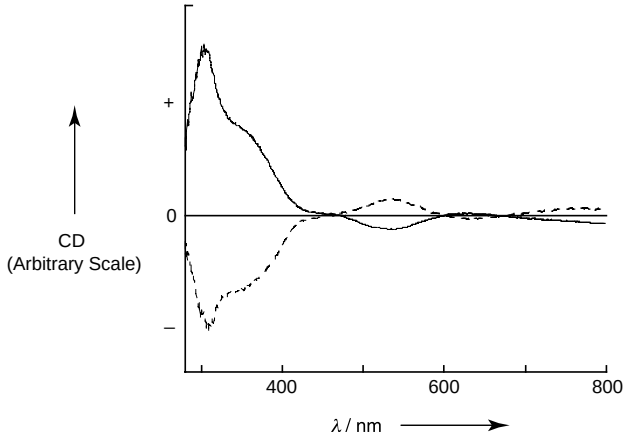

Figure 3. CD spectra of crystallites of **1** in KBr pellets. The two pellets were prepared using selected crystals, and showed enantiomeric CD patterns that provide definitive evidence that spontaneous resolution had occurred.

other, which results in a chiral (conglomerate) crystal. Enantiomeric circular dichroism (CD) spectra obtained from selected crystals provide definitive evidence that spontaneous resolution has occurred (Figure 3).

The Fe–N bond lengths for the protonated $[Fe^{II}H_3L]^{2+}$ species (Fe2 and Fe4) at 295 K range from 2.146(2) to 2.210(2) Å, which are typical values for HS Fe^{II} centers, while those at 100 K range from 2.019(2) to 2.044(2) Å, more typical for LS Fe^{II} ions. In the deprotonated $[Fe^{III}L]$ species (Fe1 and Fe3), the Fe–N bond lengths are in the range 1.974(2) to 2.023(2) Å at 295 K, and 1.926(2) to 1.996(2) Å at 100 K, both suggestive of LS Fe^{III} species. Figure 2b illustrates that there are two types of flat layers: One layer contains only $[Fe^{II}H_3L]^{2+}$ species (Fe2 and Fe4), the other layer contains only $[Fe^{III}L]$ species (Fe1 and Fe3), with both layers stacked alternately along the *c* axis.

Magnetic susceptibility measurements, Mössbauer spectra, and X-band ESR spectra provide evidence of spin-crossover in both the Fe^{II} and Fe^{III} centers. The magnetic properties are shown in Figure 4a in the form of $\chi_M T$ versus T plots, in which χ_M is the molar magnetic susceptibility and T is the absolute temperature. When the sample was warmed or cooled slowly without prior quenching at low temperature, the $\chi_M T$ value is constant at 0.4 $cm^3 K mol^{-1}$ at temperatures of 2–120 K, which is the expected spin-only value (0.38 $cm^3 K mol^{-1}$) for LS Fe^{II} ($S=0$) and LS Fe^{III} ($S=1/2$) of both the Fe^{II} ($S=0$) and Fe^{III} ($S=1/2$) sites. The $\chi_M T$ value increases rapidly in the 140 to 180 K region, which corresponds with a spin-transition at the Fe^{II} site from the LS Fe^{II} ($S=0$) to the HS Fe^{II} ($S=2$) state. The $\chi_M T$ value at 200 K was 3.6 $cm^3 K mol^{-1}$, which is in the expected range for HS Fe^{II} ($S=2$) and LS Fe^{III} ($S=1/2$) states. Above 200 K, the $\chi_M T$ value increased gradually owing to the spin transition from the LS Fe^{III} ($S=1/2$) to the HS Fe^{III} ($S=5/2$) state. X-band EPR spectroscopy indicates that the onset of the LS-to-HS transition at the Fe^{III} site occurs at around 200 K. The above data demonstrates that there are at least three accessible electronic states: LS Fe^{II}–LS Fe^{III}, HS Fe^{II}–LS Fe^{III}, and HS Fe^{II}–HS Fe^{III}. The temperature dependence of the Mössbauer spectra agreed with the magnetic susceptibility results. At 78 K, the Mössbauer spectrum consisted of two doublets exhibiting quadrupolar splitting (LS Fe^{III}: $\delta=0.20$, $\Delta E_Q=1.83$; LS Fe^{II}: $\delta=0.43$, $\Delta E_Q=0.32$ $mm s^{-1}$), which demonstrates that both the Fe^{II} and the Fe^{III} sites are in the LS state. At 140–170 K, three doublets coexist because of the existence of LS and HS Fe^{II} sites, and the LS Fe^{II} doublet disappears at 200 K. Deconvolution of the Mössbauer spectrum was performed at each temperature, and the molar fraction of the HS Fe^{II} species, measured as a function of temperature, was consistent with the magnetic susceptibility results (Figure 4b).

Considering the LS–HS switching ability of the electronic structure in the separate $[Fe^{II}H_3L]^{2+}$ and $[Fe^{III}L]$ constituents, it is clear that their supramolecular association in this mixed-valence homochiral complex not only modifies the spin-crossover of the $[Fe^{II}H_3L]^{2+}$ unit, but also triggers the spin-crossover of the otherwise low-spin $[Fe^{III}L]$ unit. Indeed,

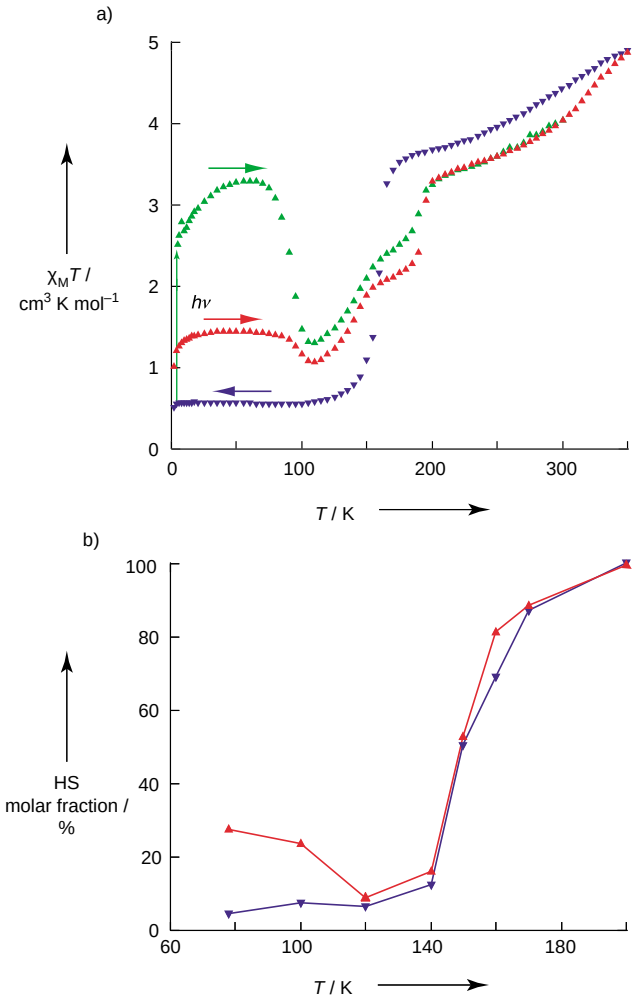

Figure 4. a) Thermal variation of $\chi_M T$ for **1** under cooling (▼) and warming (▲) modes. After quenching to 2 K, the sample was warmed (▲) and both a frozen-in effect and a two-step spin-crossover on the Fe^{II} site were observed. The ▲ symbols represent the $\chi_M T$ versus T plot that highlights the LIESST effect at 5 K and the subsequent thermal relaxation; b) the molar fraction of HS Fe^{II} versus T during cooling (▼) and warming (▲) as calculated by Mössbauer spectroscopy. When the sample was warmed after quenching to 78 K (▲), a frozen-in effect was observed.

$[Fe^{II}H_3L](NO_3)_2$ is in the HS state in its unsolvated form, and exhibits gradual spin-crossover (at 100–250 K) in its hydrated form. However, $[Fe^{III}L]\cdot 2.5\,H_2O$ is in the LS state over the entire temperature range. There must be interdependence in the LS–HS switching ability of the Fe^{II} and Fe^{III} sites. When the sample of **1** was warmed after quenching to 2 K, a "frozen-in" effect and a two-step spin-crossover at the Fe^{II} site were observed from magnetic susceptibility measurements.

Compound **1** exhibits the light-induced excited-spin-state trapping (LIESST) effect.[3] Irradiation with green light ($\lambda \approx$ 500 nm) at 5 K affords an increase in the $\chi_M T$ value, which is attributed to the spin-transition from the LS to the HS state at the Fe^{II} site. After the light is switched off, the HS Fe^{II} state is maintained at 5 K, and on warming, the thermal relaxation is complete above 100 K (Figure 4). Variable-temperature laser Raman spectroscopy[11] using an argon-ion laser ($\lambda =$ 514.5 nm) has also confirmed the LIESST effect.

Herein, we have demonstrated that a compound with bulk optical activity, spin-crossover, and mixed valency was obtained by a one-pot assembly reaction of a programmed single molecule. The conditions necessary to achieve a chiral and magnetochiral switch are thus present in this material.[12] This unprecedented combination of optical, spin-crossover, and mixed-valence properties opens up new prospects for the effective use of spin-crossover materials. For example, this chiral photochromic compound may be used in high-density optical data storage media with a nondestructive readout property. With conventional achiral optical recording media based on photochromic compounds, the data that is stored can be erased when it is exposed to the light used to read the data by UV/Vis spectroscopy (destructive readout). Our chiral material, however, provides a solution to such a problem by using an optical rotation measurement. Since the optical rotation originates from the difference in refractive indices, it can be detected at much longer wavelengths than the absorption band, and thus, we can avoid photoinduced data destruction while reading the data.

Experimental Section

1: The reaction mixture of the H_3L ligand and $Fe^{III}(NO_3)_3\cdot 9\,H_2O$ (1:1 molar ratio) in methanol was acidified with HCl and the resulting solution was allowed to stand for several days. During this time, yellow-orange crystals of $[Fe^{II}H_3L](NO_3)_2\cdot 3\,H_2O$ were obtained. An aqueous solution of NaOH was added to a warmed solution of $[Fe^{II}H_3L](NO_3)_2\cdot 3\,H_2O$ in MeOH (1.5:1 ratio). The solution was allowed to stand for several days, from which, $[Fe^{II}H_3L][Fe^{II}L](NO_3)_2$ (**1**) was obtained.

Physical measurements: Magnetic susceptibilities were measured using an MPMS5 SQUID susceptometer (Quantum Design) in the 2–350 K temperature range at a 1 K min^{-1} sweeping rate under an applied magnetic field of 1 T. For the LIESST experiment, a xenon arc lamp (Hamamatsu L7810) was used as the light source. The Mössbauer spectra were recorded by using a Wissel 1200 spectrometer and a proportional counter. A $^{57}Co(Rh)$ radioactive source was used in a constant acceleration mode. The isomer shifts are reported relative to metallic iron foil. The diffraction data were collected using an IPDS-Stoe diffractometer at 295 and 100 K. The structures were solved by direct methods and refined with full-matrix least-squares procedures using SHELXS-97. CCDC-196219 and CCDC-196220 contain the supplementary crystallographic data for this paper. These data can be obtained free of charge via www.ccdc.cam.ac.uk/conts/retrieving.html (or from the Cambridge Crystallographic Data Centre, 12 Union Road, Cambridge CB2 1EZ, UK; fax: (+44) 1223-336-033; or deposit@ccdc.cam.ac.uk).

Received: October 21, 2002 [Z50399]

Keywords: bistability · chirality · hydrogen bonds · mixed-valent compounds · spin-crossover

[1] a) L. Cambi, L. Szego, A. Cassaro, *Accad. Naz. Lincei Atti Mem. Cl. Sci. Fis. Mat. Nat. Sez. 3* **1931**, *13*, 809; b) E. König, *Prog. Inorg. Chem.* **1987**, *35*, 527; c) O. Kahn, *Molecular Magnetism*, VCH, Weinheim, **1993**.

[2] a) O. Kahn, J. C. Martinez, *Science* **1998**, *279*, 44; b) M. Irie, *Chem. Rev.* **2000**, *100*, 1685; c) M. E. Itkis, X. Chi, A. W. Cordes, R. C. Haddon, *Science* **2002**, *296*, 1443.
[3] a) S. Decurtins, P. Gütlich, C. P. Kohler, H. Spiering, A. Hauser, *Chem. Phys. Lett.* **1984**, *105*, 1; b) P. Gütlich, A. Hauser, H. Spiering, *Angew. Chem.* **1994**, *106*, 2109; *Angew. Chem. Int. Ed. Engl.* **1994**, *33*, 2024.
[4] A. Hauser, J. Jeftic, H. Romstedt, R. Hinek, H. Spiering, *Coord. Chem. Rev.* **1999**, *190–192*, 471.
[5] a) J. A. Real, E. Andres, M. C. Munoz, M. Julve, T. Granier, A. Bousseksou, F. Varret, *Science* **1995**, *268*, 265; b) P. J. van Koningsbruggen, Y. Garcia, O. Kahn, L. Fournes, H. Kooijman, A. L. Spek, J. G. Haasnoot, J. Moscovici, K. Provost, A. Michalowicz, F. Renz, P. Gütlich, *Inorg. Chem.* **2000**, *39*, 1891; c) E. Breuning, M. Ruben, J.-M. Lehn, F. Renz, Y. Garcia, V. Ksenofontov, P. Gütlich, E. Wegelius, K. Rissanen, *Angew. Chem.* **2000**, *112*, 2563; *Angew. Chem. Int. Ed.* **2000**, *39*, 2504.
[6] a) D. Boinnard, A. Bousseksou, A. Dworkin, J.-M. Savariault, F. Varret, J. P. Tuchagues, *Inorg. Chem.* **1994**, *33*, 271; b) J.-F. Letard, J. A. Real, N. Moliner, A. B. Gaspar, L. Capes, O. Cador, O. Kahn, *J. Am. Chem. Soc.* **1999**, *121*, 10630.
[7] a) S. Hayami, Z. Gu, M. Shiro, Y. Einaga, A. Fujishima, O. Sato, *J. Am. Chem. Soc.* **2000**, *122*, 7126; b) S. Hayami, Z. Gu, H. Yoshiki, A. Fujishima, O. Sato, *J. Am. Chem. Soc.* **2001**, *123*, 11644.
[8] a) I. Katsuki, Y. Motoda, Y. Sunatsuki, N. Matsumoto, T. Nakashima, M. Kojima, *J. Am. Chem. Soc.* **2002**, *124*, 629; b) Y. Sunatsuki, Y. Motoda, N. Matsumoto, *Coord. Chem. Rev.* **2002**, *226*, 199.
[9] J. Jacques, A. Collet, S. H. Wilen, *Enantiomers, racemates and resolutions*, Wiley, New York, **1981**.
[10] Crystal data at $T = 295$ K: $Mo_{K\alpha}$ ($\lambda = 0.71073$ Å), $C_{36}H_{45}N_{22}O_6Fe_2$, $M_r = 993.64$, dimensions $0.35 \times 0.35 \times 0.25$ mm, trigonal, space group $P\bar{3}$, $a = b = 11.9138(9)$, $c = 18.9783(15)$ Å, $V = 2332.9(3)$ Å^3, $Z = 2$, $\rho_{calcd} = 1.415$ g cm^{-3}, $\mu = 0.690$ mm^{-1}, 18316 reflections collected, 5959 independent reflections, wR(all) = 0.0864, R(all) = 0.0435; Fe1-N1 2.023(2), Fe1-N2 1.985(2), Fe2-N5 2.146(2), Fe2-N6 2.210(2), Fe3-N9 2.021(2), Fe3-N10 1.974(2), Fe4-N13 2.172(3), Fe4-N14 2.196(2) Å. Crystal data at $T = 100$ K, trigonal, space group $P\bar{3}$, $a = b = 11.6475(9)$, $c = 18.7992(16)$ Å, $V = 2208.7(3)$ Å^3, $Z = 2$, $\rho_{calcd} = 1.494$ g cm^{-3}, $\mu = 0.729$ mm^{-1}, 17219 reflections collected, 5603 independent reflections, wR(all) = 0.0679, R(all) = 0.0361, Fe1-N1 1.9963(15), Fe1-N2 1.9268(16), Fe2-N5 2.0279(19), Fe2-N6 2.0263(16), Fe3-N9 1.9908(15), Fe3-N10 1.9262(15), Fe4-N13 2.0439(18), Fe4-N14 2.0192(16) Å.
[11] N. Suemura, M. Ohama, S. Kaizaki, *Chem. Commun.* **2001**, 1538.
[12] P. Gütlich, Y. Garcia, T. Woike, *Coord. Chem. Rev.* **2001**, *219–221*, 839.

